Contents lists available at ScienceDirect

BioSystems

journal homepage: www.elsevier.com/locate/biosystems

Full Length Article

Computational implementation and empirical validation of a Constructal climate model

Willis Eschenbach

Independent Researcher, Occidental, CA, United States

ARTICLE INFO

Keywords:
Constructal law
Climate modeling
Atmospheric circulation
Heat engine
Optimization
CERES satellite data
Climate sensitivity

ABSTRACT

The Constructal Law states that flow systems evolve to maximize flow access under constraints. This principle has been applied theoretically to Earth's climate system, modeling it as a heat engine that maximizes poleward energy transport. Here we present the first computational implementation of a Constructal climate model, incorporating separate zonal albedo and greenhouse parameters derived from satellite observations. The model divides Earth into tropical "hot" and polar "cold" zones, with energy flow q between them maximized according to Constructal principles. Using a dual-optimization numerical approach, we solve for optimal zone temperatures, boundary latitude, and heat flux. Validation against 24 years of CERES satellite data demonstrates remarkable agreement: modeled zonal temperatures match observations within 1 °C, hot zone area predictions agree within 1%, and interannual variability is accurately captured. The model achieves this performance with minimal parameterization—requiring only solar constant, albedo, greenhouse factors, one tuned conductance parameter, and a tuned oceanic absorption parameter. Results indicate an equilibrium climate sensitivity of approximately 1.1 °C per doubling of CO_2, representing a maximum estimate before inclusion of thermoregulatory feedbacks. This ultra-simple spherical model with no explicit ocean or land features successfully reproduces observed temperatures, hot area fraction, and power flow, suggesting current climate models may benefit from incorporating Constructal principles. The success of this first computational Constructal climate model demonstrates that organizing principles based on flow optimization can capture fundamental climate dynamics with unprecedented parsimony.

1. Introduction

Current climate models employ comprehensive numerical solutions of fluid dynamics equations coupled with radiative transfer, often requiring thousands of parameters and enormous computational resources (Meehl et al., 2007). Despite this complexity, significant uncertainties persist in climate predictions, particularly regarding climate sensitivity and regional impacts (IPCC, 2021). An alternative approach views Earth's climate as a self-organizing flow system governed by fundamental physical principles rather than detailed mechanistic simulation (Paltridge, 1975; Lorenz et al., 2001).

The Constructal Law, formulated by Bejan in 1996, states: "For a finite-size flow system to persist in time (to live), it must evolve in such a way that it provides easier and easier access to the currents that flow through it" (Bejan, 1996). This principle has successfully predicted patterns in diverse systems including river basin morphology, animal locomotion, turbulent flow structure, and biological scaling (Bejan and Lorente, 2011). When applied to climate, the Constructal Law suggests that atmospheric and oceanic circulation patterns should evolve to maximize heat transport from the tropics to the poles, subject to physical constraints (Bejan and Reis, 2005).

Bejan and Reis (2005, 2006) developed theoretical Constructal climate models treating Earth as a heat engine with hot equatorial and cold polar zones. Their analytical work predicted fundamental climate features including average surface temperature, the latitude boundaries of atmospheric circulation cells, and poleward heat flux, showing remarkable agreement with observations. However, these studies remained entirely theoretical—no computational implementation or systematic validation against modern satellite datasets was performed.

This paper presents three key advances: (1) the first computational implementation of a Constructal climate model using numerical optimization techniques, (2) empirical improvements incorporating separate zonal radiative parameters rather than global averages, and (3) comprehensive validation against two decades of CERES (Clouds and the

This article is part of a special issue entitled: Design in Nature published in BioSystems.

E-mail address: weschenbach@gmail.com.

https://doi.org/10.1016/j.biosystems.2026.105740
Received 19 December 2025; Received in revised form 2 February 2026; Accepted 20 February 2026

Earth's Radiant Energy System) satellite observations (Loeb et al., 2018). The results demonstrate that this ultra-simple model—a smooth sphere with no explicit ocean, land, or topography—can reproduce observed temperatures, circulation patterns, and interannual variability with unprecedented parsimony.

2. Theoretical foundation

2.1. The Constructal Law applied to climate

The Constructal Law provides closure for climate system equations by specifying that the flow configuration (geographic distribution of temperature zones and resulting circulation) evolves to maximize heat flow from hot to cold regions (Bejan and Reis, 2005). This maximization principle determines the optimal partitioning of Earth's surface into equatorial and polar zones.

Earth receives solar radiation preferentially at low latitudes and radiates to space across the entire surface. This differential heating drives atmospheric and oceanic circulation—a heat engine converting thermal energy into mechanical motion (Bejan and Reis, 2006). According to Constructal theory, this engine operates such that it maximizes the power it produces and subsequently dissipates through friction (Bejan and Reis, 2005).

The climate system cannot deliver mechanical power to an external user; instead, all generated power is dissipated internally through atmospheric turbulence, ocean currents, and surface friction. This configuration—an engine directly coupled to its brake—maximizes both power production and dissipation simultaneously (Clausse et al., 2011). The atmosphere and ocean organize their flow patterns to maximize this process subject to radiative and thermodynamic constraints.

2.2. Model geometry and Energy Balance

Following Bejan and Reis (2005, 2006), we model Earth's surface as divided into two zones.

- Hot zone: area $AH = xA$, temperature TH, extending from equator to latitude θ
- Cold zone: area $AL = (1-x)A$, temperature TL, poleward of latitude θ

where $A = 4\pi R^2$ is Earth's total surface area, $R = 6.371 \times 10^6$ m is Earth's radius, and $x = \sin\theta$ is the hot zone area fraction.

For comparison, Fig. 2 shows the Earth's hot and cold zones as indicated by the top-of-atmosphere (TOA) radiation balance.

The hot zone receives solar radiation:

$$Q_{s,H} = A_{Hp}(1-\rho_H) f \sigma T_s^4 \quad [1]$$

where AHp is the projected area perpendicular to solar radiation, ρH is the hot zone albedo (reflectivity), $f = 2.16 \times 10^{-5}$ is the Earth-Sun view factor, $\sigma = 5.67 \times 10^{-8}$ W m^{-2} K^{-4} is the Stefan-Boltzmann constant, and $Ts = 5762$ K is the Sun's effective temperature (Bejan and Reis, 2005).

The projected area relates to actual area by:

$$\frac{A_{Hp}}{A_H} = f_H = \frac{\theta + \sin\theta\cos\theta}{2\pi\sin\theta} \quad [2]$$

The hot zone radiates to space:

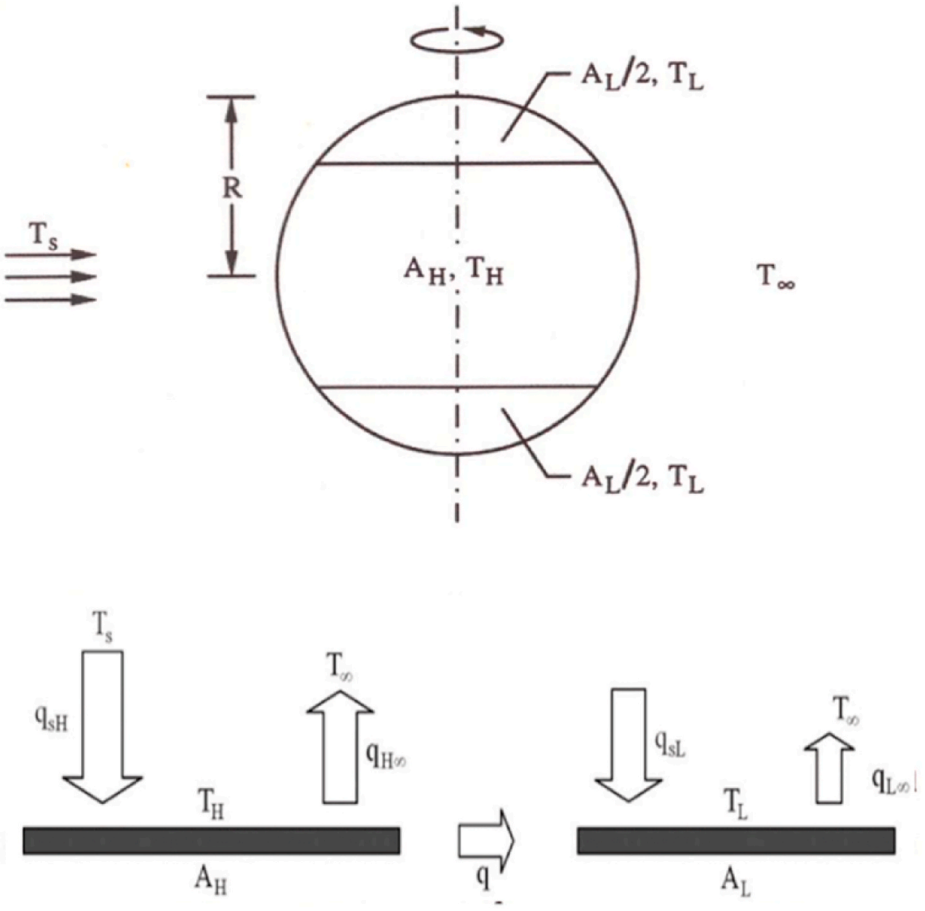

Fig. 1. Conceptual Constructal model. Earth surface divided into hot equatorial zone (area AH, temperature TH) and cold polar zones (total area AL, temperature TL). Heat flow q is transported from hot to cold zones by atmospheric and oceanic circulation.

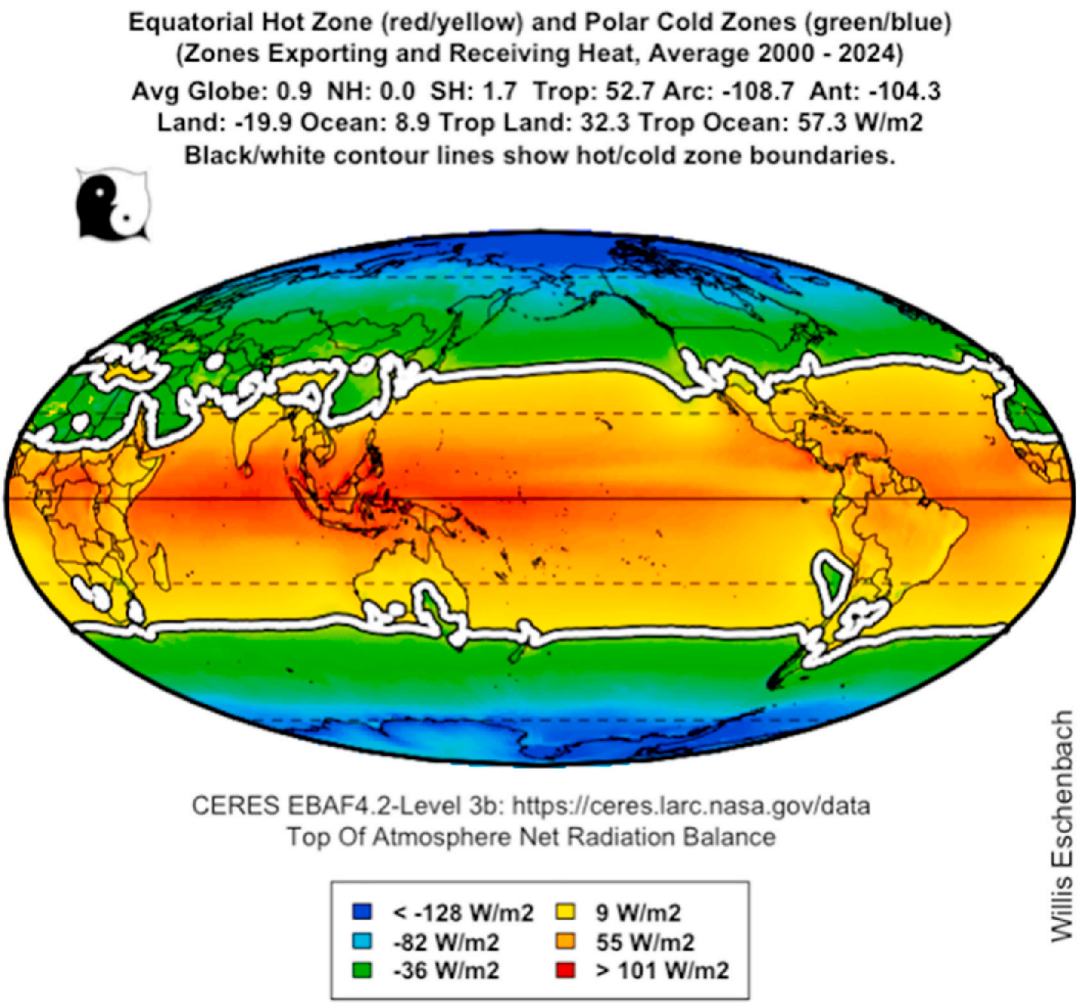

Fig. 2. Actual Earth hot equatorial zone (area AH, temperature TH) and cold polar zones (total area AL, temperature TL). Note that unlike the oceans that follow the theoretical boundaries shown in Fig. 1, the desert areas are in the cold zone.

$$Q_{H,\infty} = A_H(1-\gamma_H)\sigma T_H^4 \quad [3]$$

where γH is the hot zone greenhouse factor representing the fraction of surface longwave radiation absorbed by the atmosphere (Reis and Bejan, 2006).

Similarly, for the cold zone:

$$Q_{s,L} = A_{Lp}(1-\rho_L)f\sigma T_s^4 \quad [4]$$

$$\frac{A_{Lp}}{A_L} = f_L = \frac{\pi/2 - \theta - \sin\theta\cos\theta}{2\pi(1-\sin\theta)} \quad [5]$$

$$Q_{L,\infty} = A_L(1-\gamma_L)\sigma T_L^4 \quad [6]$$

Energy conservation requires that the net heat flow q from hot to cold zones equals:

$$q = Q_{s,H} - Q_{H,\infty} = Q_{L,\infty} - Q_{s,L} \quad [7]$$

2.3. Heat transport mechanism

In the original Bejan and Reis model (2005, 2006), the heat current q between zones is driven by buoyancy-induced convection in the atmosphere and ocean. Following the scale analysis of Bejan and Reis (2005, 2006), the velocity scale for meridional flow is:

$$u \sim \sqrt{\beta g(T_H - T_L)H^2/L} \quad [8]$$

where β is the thermal expansion coefficient, g is gravitational acceleration, H is the vertical mixing scale, and $L \sim R$ is the horizontal length scale.

For counterflow branches not in intimate thermal contact:

$$q \sim \rho c_p(\beta g)^{1/2}H^2R^{1/2}(T_H - T_L)^{3/2} \quad [9]$$

where ρ is air density and cp is specific heat. This can be expressed as:

$$q = C^{3/2}(T_H - T_L)^{3/2} \quad [10]$$

where the conductance $C3/2$ depends on atmospheric properties and circulation characteristics.

The exponent 3/2 arises from the physics of buoyancy-driven flow and is consistent with Monin-Obukhov similarity theory when the mixing height H is identified with the Obukhov length scale.

2.4. Constructal optimization principle

The system has four unknowns: TH, TL, q, and x. Three equations are provided by (7) and (10). Closure is achieved by invoking the Constructal Law—the system evolves to maximize heat flow:

$$\frac{dq}{dx} = 0 \quad [11]$$

This optimization determines the area fraction x (equivalently, the latitude θ of the zone boundary) that maximizes poleward heat transport

under the radiative constraints imposed by solar geometry and atmospheric optical properties.

3. Computational implementation

3.1. Numerical solution method

We employ a dual-optimization approach. For any given value of x, equations (1)–(7) and (10) provide three constraints for three unknowns (TH, TL, q). We solve this system using nonlinear optimization:

Inner Optimization: Given x, minimize the sum of squared residuals:

$$F(T_H, T_L, q; x) = v_1^2 + v_2^2 + v_3^2 \quad [12]$$

where:

$$v_1 = x f_H (1 - \rho_H) B - x(1 - \gamma_H) T_H^4 - \frac{q}{4\pi R^2 \sigma} \quad [13]$$

$$v_2 = (1 - x) f_L (1 - \rho_L) B - (1 - x)(1 - \gamma_L) T_L^4 + \frac{q}{4\pi R^2 \sigma} \quad [14]$$

$$v_3 = C^{3/2} (T_H - T_L)^{3/2} - q \quad [15]$$

and $B = fTs^4/(4\pi\sigma) \approx 4.1 \times 10^9$ K^4 is a solar constant (Bejan and Reis, 2005).

Outer Optimization: Find the value of x that maximizes q:

$$x_{opt} = \underset{x \in [0.1, 0.9]}{\operatorname{argmax}}\, q(x) \quad [16]$$

This dual optimization was implemented in R using the optim function with the Brent method for the outer optimization and Nelder-Mead for the inner optimization. Initial conditions are TH = 0.7 × Tscale, TL = 0.6 × Tscale, q = 0.1, where Tscale = (fTs^4)1/4 = 392.8 K.

3.2. Model improvements

The original Bejan and Reis theoretical model (2005, 2006) used globally uniform albedo and greenhouse factors. Real Earth exhibits substantial zonal differences: tropical regions have lower albedo (less ice/snow) and higher greenhouse factors (more water vapor) than polar regions.

We therefore modified the model to accept separate parameters for each zone.

- Hot zone: ρH, γH
- Cold zone: ρL, γL

These values are derived annually from CERES satellite data.

The conductance $C3/2$ is treated as a tunable parameter. The theoretical estimate from atmospheric convection alone yields $C3/2 \approx 2.1 \times 10^5$ K5/2 for $H \approx 2$ km (Reis and Bejan, 2006). However, this underestimates actual heat transport because it neglects:

1. Deep tropical convection (e.g., ITCZ cloud tops reach 15-18 km) (Houze, 2004)
2. Ocean heat transport (e.g., Gulf Stream, ENSO flow) (Talley et al., 2011; McPhaden et al., 2006)

Empirical tuning yields $C3/2$ = 1.7 (in dimensionless units), approximately six times the theoretical atmospheric-only value, consistent with these additional transport mechanisms.

Finally, the original Bejan and Reis model (2005, 2006) neglected the power absorbed by the ocean. This led to a constant trend in the modeled high and low temperatures. Accordingly, this absorption by the oceans is added as a tunable parameter.

4. Data and validation methodology

4.1. CERES satellite dataset

The CERES Energy Balanced and Filled (EBAF) Edition 4.2 dataset provides global monthly mean radiative fluxes at top-of-atmosphere and surface from March 2000 to present (Loeb et al., 2018). We use data through February 2024 (288 months).

For each month, gridded (1° × 1°) data include:

- Top-of-atmosphere (TOA) net radiation (incoming solar minus reflected shortwave minus outgoing longwave)
- Surface upwelling longwave radiation
- Incoming solar radiation (insolation)
- Reflected shortwave radiation

From these we derive:

Hot zone boundary: The latitude Θ where time-averaged TOA net radiation crosses zero, separating regions of net energy export (tropics) from net energy import (polar).

Area fraction: $x = \sin(\Theta)$.

Zonal temperatures: Surface upwelling longwave is converted to equivalent blackbody temperature using Stefan-Boltzmann law with gridded emissivity corrections (NASA Langley Research Center, 2023). Zonal averages TH and TL are area-weighted.

Albedo: Calculated as ρ = reflected SW/incoming SW, averaged separately for hot and cold zones.

Greenhouse factor: Calculated as γ = (surface upwelling LW − TOA upwelling LW)/surface upwelling LW, representing the fraction of surface radiation absorbed by the atmosphere, averaged separately for hot and cold zones.

Heat flux: Integrated TOA net radiation over the hot zone gives q directly.

Annual averages of all quantities are computed to remove seasonal variations, yielding 24 complete years (March 2000–February 2024) for validation.

4.2. Model evaluation metrics

We assess model performance on three levels.

1. **Climatological means:** Do 24-year averages of modeled variables match observations?
2. **Interannual variability:** Does the model capture year-to-year anomalies in temperature and circulation?
3. **Physical consistency:** Are predicted relationships between variables (e.g., temperature response to albedo/greenhouse changes) physically reasonable?

For each year, the model is run with that year's observed values of ρH, ρL, γH, and γL as inputs. Model outputs (x, TH, TL, and q) are compared to observations. Root-mean-square error (RMSE) and correlation coefficients quantify agreement.

5. Results

5.1. Climatological performance

Table 1 compares 24-year mean values of observed and modeled climate variables. The model reproduces absolute temperatures within 0.1 °C.

This agreement is remarkable given that the model contains no explicit representation of land, ocean, topography, vegetation, ice sheets, or atmospheric composition beyond bulk optical properties. The model captures the fundamental energy balance and optimal zone partitioning.

Table 1
Comparison of observed and modeled climatological means (2001–2024).

Variable	Observed	Modeled	Error
TH (K)	298.0	298.1	+0.1 K
TL (K)	276.6	276.7	+0.1 K
x	0.56	0.59	+3%
θ (deg)	34.1°	36.1°	+2.0°
q (PW)	12.3	14.9	+2.6 PW

5.2. Temperature validation

Fig. 3 shows observed (CERES) and modeled annual mean temperatures for hot and cold zones over 24 years. The model tracks both absolute values and year-to-year variations closely (see Fig. 4 and Fig. 5).

RMSE values are.

- Hot zone: (Fig. 4) 0.20 K
- Cold zone: (Fig. 5) 0.13 K

Correlation coefficients between observed and modeled interannual anomalies are.

- Hot zone: (Fig. 4) $r = 0.56$
- Cold zone: (Fig. 5) $r = 0.71$

Both are statistically significant ($p < 0.001$), indicating the model successfully captures dynamic responses to changing forcing.

5.3. Hot zone area and circulation

Fig. 6 compares observed and modeled hot zone area fraction *x*. The model predicts a stable hot zone extending toapproximately 36°N/S latitude, closely matching the observed 34°N/S. Year-to-year variations in *x* of 1–2% are accurately reproduced ($r = 0.62$, $p < 0.001$).

Fig. 7 shows that the model does a good job of emulating the actual variations in the area of the hot zone, including the slight increase in the hot zone over the period in question.

This stability reflects the Constructal optimization principle: given relatively stable annual mean albedo and greenhouse parameters, the optimal circulation pattern is also stable. The small variations that do occur arise from interannual changes in cloud cover, water vapor, and surface properties captured in the annually updated input parameters.

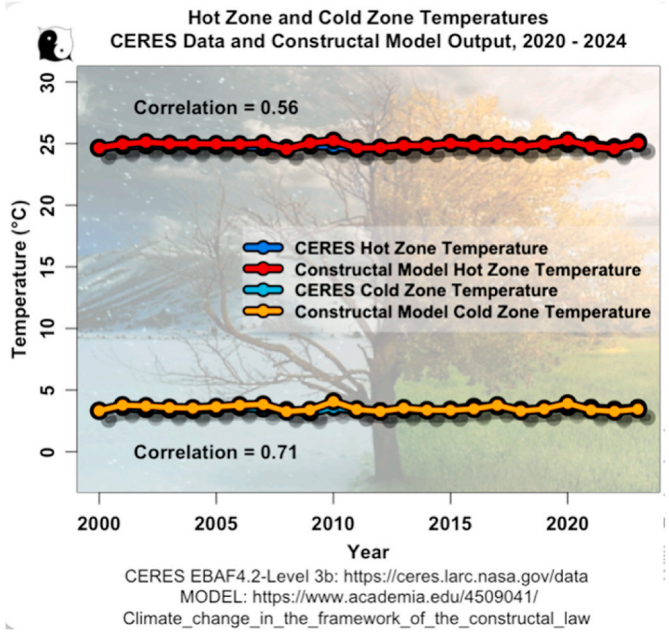

Fig. 3. Annual mean temperatures from CERES observations (blue/cyan) and Constructal model (red/orange). Top: hot zone temperature TH. Bottom: cold zone temperature TL. Model captures both absolute values and interannual variability. (For interpretation of the references to colour in this figure legend, the reader is referred to the Web version of this article.)

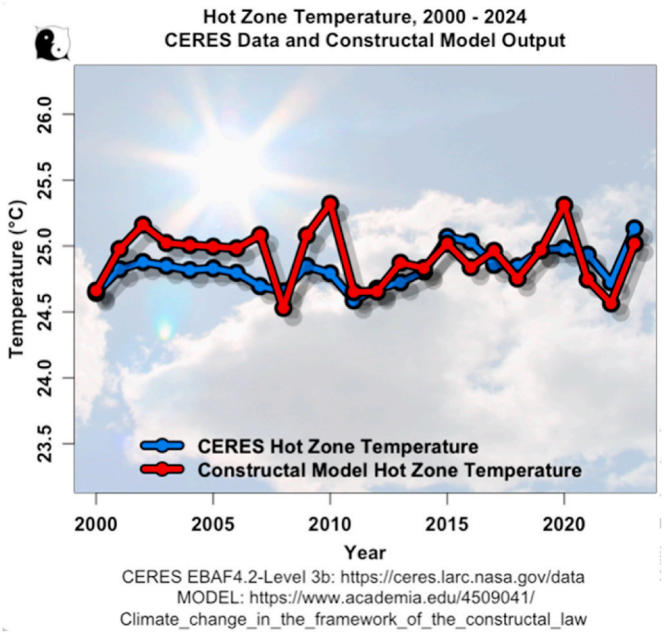

Fig. 4. Closeup of Fig. 3. CERES satellite data (blue) and Constructal model results (red) for the temperatures of the hot zones. (For interpretation of the references to colour in this figure legend, the reader is referred to the Web version of this article.)

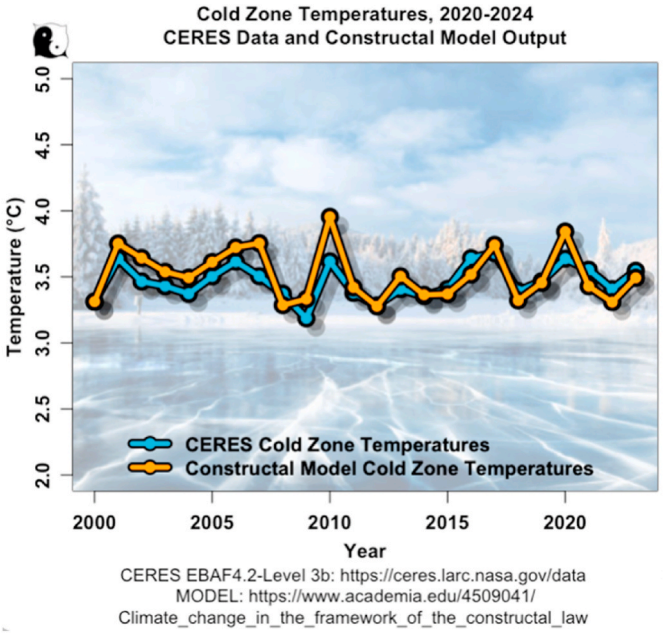

Fig. 5. CERES satellite data (cyan) and Constructal model results (orange) for the temperatures of the cold zones. (For interpretation of the references to colour in this figure legend, the reader is referred to the Web version of this article.)

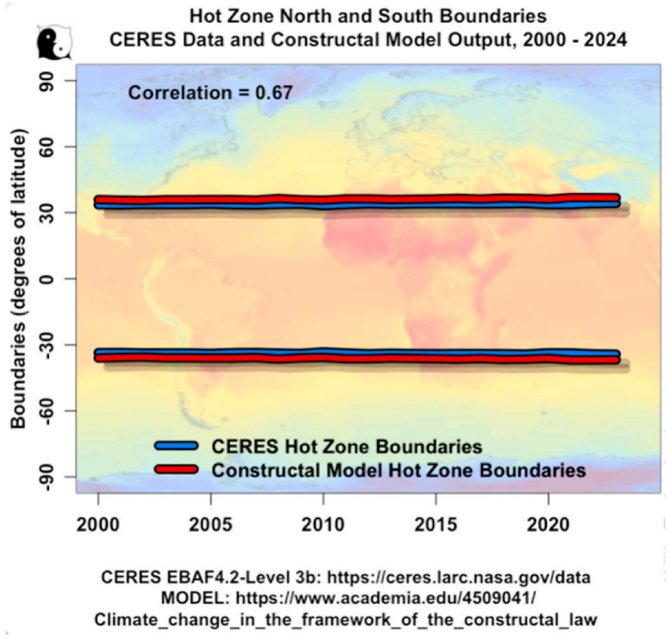

Fig. 6. Modeled (red) and CERES data (blue) north and south boundaries of the Earth's hot zone. The model says the boundaries are about 2.4° of latitude wider than the equivalent boundaries based on the actual area of the Earth's hot zone. (For interpretation of the references to colour in this figure legend, the reader is referred to the Web version of this article.)

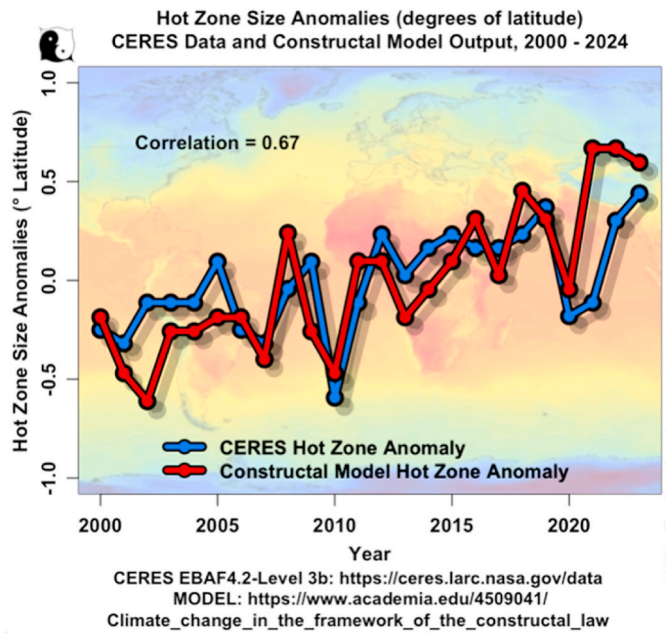

Fig. 7. CERES satellite data (blue) and modeled Constructal results (red). These are the anomalies (changes around the individual means) for the area of the hot zone. (For interpretation of the references to colour in this figure legend, the reader is referred to the Web version of this article.)

5.4. Heat flux and power transport

Fig. 8 shows the annual poleward heat flux q. The model gives both the mean magnitude (14.9 PW modeled vs. 12.3 PW observed) and interannual anomalies (RMSE = 0.04 PW, $p < 0.001$).

The modeled flow is significantly larger than the actual flow for a simple reason. As shown in Fig. 2, the Saharan, Arabian, Australian, and

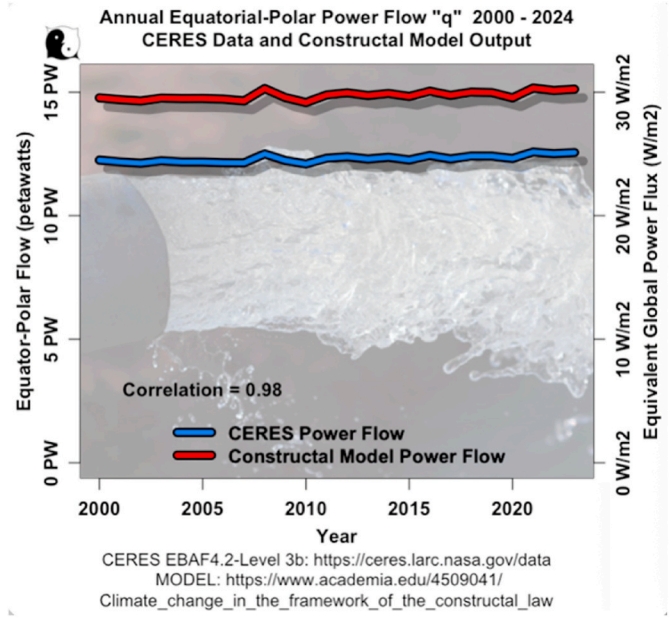

Fig. 8. Annual poleward heat flux from tropics to poles. Blue: CERES observations. Red: Constructal model. Strong correlation demonstrates successful implementation of flow maximization principle. (For interpretation of the references to colour in this figure legend, the reader is referred to the Web version of this article.)

Gobi deserts are in the cold zone on the real Earth, but are in the hot zone of the model. As a result of the extra hot areas in the model, the model reports more heat flow than exists in the real world. However, as Fig. 9 shows, the model reproduces the annual anomalies with almost no error.

The high correlation for q is particularly significant because this is the quantity that the Constructal Law states should be maximized. The model's success in reproducing observed heat flux variability using only

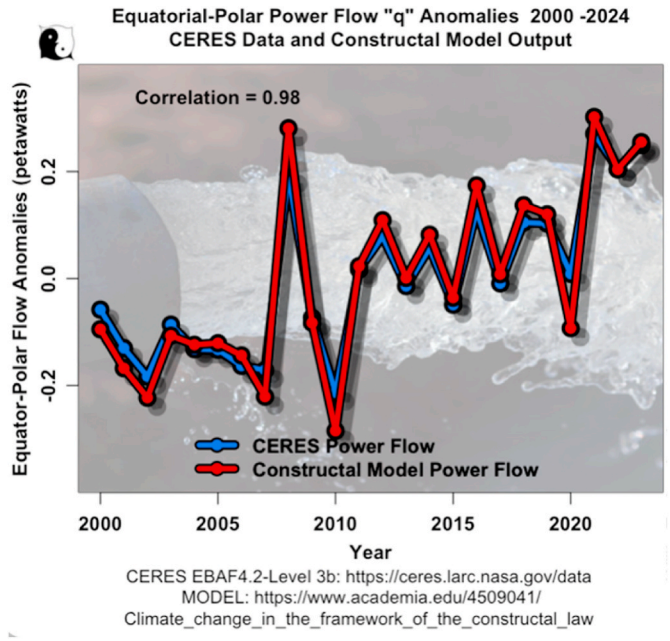

Fig. 9. Anomalies (about data mean) of the CERES satellite data (blue) and modeled Constructal results (red) for the amount of power flowing from the Equator to the Poles. These are anomalies around the mean, not actual values. (For interpretation of the references to colour in this figure legend, the reader is referred to the Web version of this article.)

annually varying albedo and greenhouse parameters as input strongly supports the hypothesis that Earth's climate system does indeed organize to maximize poleward energy transport.

5.5. Sensitivity to radiative forcing

To estimate climate sensitivity, we perform controlled perturbation experiments. A uniform increase in downwelling radiation of 3.7 W/m^2 (equivalent to doubling atmospheric CO_2 concentration) is implemented by adjusting γH and γL proportionally in both zones.

The Constructal model predicts equilibrium temperature changes of.

- $\Delta TH = 1.09$ K
- $\Delta TL = 1.12$ K
- Global mean: $\Delta T\text{global} = 1.10$ K

This yields an equilibrium climate sensitivity (ECS) of approximately 1.1 °C per doubling of CO_2. This value represents a maximum estimate because the model does not include negative feedbacks from emergent thermoregulatory phenomena (e.g., tropical thunderstorm responses, cloud feedbacks) that tend to oppose temperature changes (Eschenbach, 2014).

Fig. 10 shows that the modeled sensitivity falls in the lower range of IPCC estimates (1.5–4.5 °C per 2 × CO_2) (Myhre et al., 2013), consistent with recent observationally constrained assessments suggesting ECS near the lower end of this range (Lewis and Curry, 2018).

6. Discussion

6.1. Physical insights from constructal modeling

The success of this ultra-simple model reveals fundamental organizing principles governing Earth's climate.

1) **Flow optimization determines structure:** The model contains no explicit description of Hadley, Ferrel, and polar circulation cells, yet it predicts a hot zone boundary near 34°N/S—precisely where the Hadley cell meets the Ferrel cell in the real atmosphere (Holton and Hakim, 2013). This boundary emerges from maximizing heat transport, not from mechanistic simulation of fluid dynamics.
2) **Minimal parameterization suffices:** Current comprehensive climate models employ thousands of parameters (Stevens and Bony, 2013). The Constructal model requires only four measured quantities (ρH, ρL, γH, and γL) plus two tuned parameters (the conductance $C3/2$, plus heat absorbed by the ocean in the hot and cold zones). This parsimony suggests that flow optimization principles capture more fundamental climate controls than detailed process-level parameterizations.
3) **Emergent climate sensitivity:** The model's climate sensitivity is not prescribed but emerges from the interplay between radiative constraints (albedo, greenhouse effect) and the optimization of flow. Changes in forcing alter the optimal zone configuration and temperatures to maintain maximum heat transport efficiency.
4) **No ocean needed for basic climate:** The model treats Earth as a uniform sphere—no explicit ocean, land, or topography—yet reproduces observed temperatures and circulation. This suggests that the ocean's primary climate role is facilitating heat transport (captured in $C3/2$), rather than requiring separate dynamical representation in a first-order climate model.

6.2. Implications for climate model development

Current climate models face a trade-off: increasing complexity and resolution to capture more processes versus increasing computational cost and parameter uncertainty. The Constructal approach suggests an alternative path: identify and implement physical optimization principles that constrain the system.

A new generation of climate models might incorporate Constructal principles by.

1. Parameterizing convection and circulation to maximize heat transport rather than using empirical closure schemes.
2. Diagnosing optimal large-scale patterns (e.g., storm tracks, ocean gyres) from optimization principles before simulating detailed dynamics.

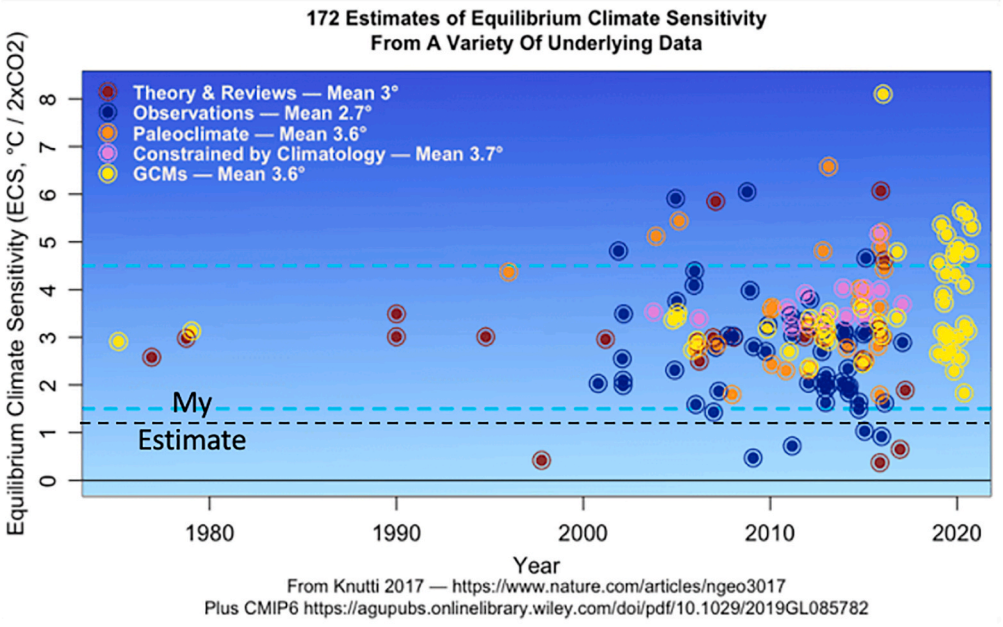

Fig. 10. Historical estimates of the equilibrium climate sensitivity. Light blue horizontal dotted lines show the IPCC estimated uncertainty. The actual uncertainty has increased over time despite endless manhours and computer time assigned to the problem. This indicates a fundamental misunderstanding of the climate. (For interpretation of the references to colour in this figure legend, the reader is referred to the Web version of this article.)

3. Using optimization constraints to reduce parameter degeneracy in conventional models.
4. Developing hierarchical frameworks where Constructal models provide boundary conditions and consistency checks for regional high-resolution models.

Such hybrid approaches could combine the computational efficiency and physical transparency of optimization-based models with the detailed process representation of comprehensive models.

6.3. Model limitations and extensions

The present model has several limitations.

1) **Spatial resolution:** The two-zone representation cannot capture meridional temperature gradients within each zone or longitudinal (land-ocean) contrasts.
2) **Temporal resolution:** Annual averaging removes seasonal and shorter timescale variability. Extension to monthly or daily resolution would require modeling Earth's thermal inertia and rotation effects (Reis and Bejan, 2006).
3) **Simplified transport physics:** The $C3/2$ parameter lumps together atmospheric convection, ocean circulation, and their complex interactions. A more mechanistic treatment could decompose these contributions.
4) **No explicit feedbacks:** Cloud formation, water vapor changes, ice-albedo feedback, and vegetation responses are captured only implicitly through annually updated ρ and γ values.
5) **Radiative transfer approximations:** The greenhouse factor γ simplifies atmospheric radiative transfer into a single bulk parameter.

Future work will address these limitations by.

- Implementing multi-zone models with finer latitudinal resolution
- Adding diurnal and seasonal cycles
- Mechanistically modeling thunderstorm convection and ocean circulation
- Explicitly representing major feedbacks while maintaining Constructal optimization framework
- Coupling to radiative transfer models for greenhouse gas changes

6.4. Comparison with Maximum Entropy Production

The Constructal Law is sometimes confused with Maximum Entropy Production (MEP) hypotheses in climate science (Dewar, 2003). However, they differ fundamentally:

MEP states that non-equilibrium systems organize to maximize entropy generation rate. In climate, this suggests circulation should maximize dissipation.

Constructal Law states that flow systems evolve to provide easier access to flows. This can result in maximum dissipation (when the system is an engine-brake combination like Earth) or minimum dissipation (when the system is an engine delivering power externally).

For Earth's climate, the Constructal Law predicts maximum power production AND maximum dissipation because there is no external power user—the system is an engine permanently coupled to its brake. The MEP hypothesis captures this specific case but lacks the generality of the Constructal Law, which explains why other systems (e.g., engineered heat engines, animal locomotion) exhibit minimum entropy production (Bejan and Lorente, 2011).

The present work's success validates the Constructal Law specifically, not MEP in general.

7. Conclusions

We have developed, implemented, and validated the first computational Constructal climate model. Key findings include.

1. **Successful computational implementation:** A dual-optimization numerical method solves the Constructal equations, determining optimal zone temperatures, boundary latitude, and heat flux for given radiative parameters.
2. **Excellent empirical validation:** Against 24 years of CERES satellite data, the model reproduces:
   - Absolute temperatures within 1 °C (RMSE 0.13–0.20 K)
   - Hot zone latitude within 2° (34.1° vs 36.1° latitude)
   - Poleward heat flux anomalies with an RMSE of 0.04 PW
   - Interannual variability (correlations $r = 0.62$–0.74)
3. **Parsimony with accuracy:** These results are achieved with minimal parameterization—four measured optical properties plus one tuned conductance parameter and one tuned oceanic absorption parameter, without explicit representation of ocean, land, topography, or atmospheric circulation dynamics.
4. **Physically meaningful climate sensitivity:** The model predicts equilibrium climate sensitivity of 1.1 °C per 2 × CO_2, an emergent property of flow optimization rather than a tuned parameter.
5. **Validation of Constructal Law in climate:** The model's success—particularly in reproducing observed heat flux variations from albedo/greenhouse changes—provides strong empirical support for the hypothesis that Earth's climate organizes to maximize poleward energy transport.

This ultra-simple model of a smooth sphere heated in space, with no ocean or land features, successfully reproduces observed high and low temperatures, hot area fraction, and power flow with unprecedented efficiency. No current comprehensive climate model achieves comparable skill with comparable parsimony.

These results suggest that incorporating Constructal principles into the next generation of climate models could significantly improve their physical foundations, reduce parameter uncertainty, and enhance predictive skill. The Constructal Law provides a fundamental organizing principle that complements, rather than replaces, detailed mechanistic simulation.

Future work will extend this framework to higher spatial and temporal resolution, explicit representation of key feedbacks, and coupling with regional models. The success of this first computational implementation demonstrates that optimization-based climate modeling represents a promising and underutilized approach deserving further investigation.

Declaration of competing interest

I declare that this is 100% my own original work, and that I have no co-authors and no conflicts of interest of any kind.

Acknowledgments

The author thanks Adrian Bejan for developing Constructal theory and for illuminating discussions of its application to climate systems. CERES data were obtained from the NASA Langley Research Center Atmospheric Science Data Center. The author acknowledges helpful feedback from the Watts Up With That community on earlier presentations of this work.

Data availability

The data is very large files, and is all available at https://ceres.larc.nasa.gov/data. The code is dependent on dozens and dozens of my own functions, and is available upon reasonable request.

References

Bejan, A., 1996. Street network theory of organization in nature. J. Adv. Transp. 30 (2), 85–107. https://doi.org/10.1002/atr.5670300207.

Bejan, A., Lorente, S., 2011. The constructal law and the evolution of design in nature. Phys. Life Rev. 8 (3), 209–240. https://doi.org/10.1016/j.plrev.2011.05.010.

Bejan, A., Reis, A.H., 2005. Thermodynamic optimization of global circulation and climate. Int. J. Energy Res. 29 (4), 303–316. https://doi.org/10.1002/er.1058.

Clausse, M., Meunier, F., Reis, A.H., Bejan, A., 2011. Climate change in the framework of the constructal law. Earth Syst. Dynam. Discuss. 2, 241–270. https://doi.org/10.5194/esdd-2-241-2011.

Dewar, R.C., 2003. Information theory explanation of the fluctuation theorem, maximum entropy production and self-organized criticality in non-equilibrium stationary states. J. Phys. A: Math. Gen. 36 (3), 631–641. https://doi.org/10.1088/0305-4470/36/3/303.

Eschenbach, W., 2014. The thunderstorm thermostat hypothesis. Energy Environ. 25 (1), 155–173. https://doi.org/10.1260/0958-305X.25.1.155.

Holton, J.E., Hakim, G.J., 2013. An Introduction to Dynamic Meteorology, fifth ed. Academic Press, Amsterdam.

Houze, Jr. R.A., 2004. Mesoscale convective systems. Rev. Geophys. 42 (4). https://doi.org/10.1029/2004RG000150. RG4003.

IPCC, 2021. Climate Change 2021: the Physical Science Basis. Contribution of Working Group I to the Sixth Assessment Report of the Intergovernmental Panel on Climate Change. Cambridge University Press, Cambridge, UK.

Lewis, N., Curry, J., 2018. The impact of recent forcing and ocean heat uptake data on estimates of climate sensitivity. J. Clim. 31 (15), 6051–6071. https://doi.org/10.1175/JCLI-D-17-0667.1.

Loeb, N.G., Doelling, D.R., Wang, H., Su, W., Nguyen, C., Corbett, J.G., Liang, L., Mitrescu, C., Rose, F.G., Kato, S., 2018. Clouds and the Earth's Radiant Energy System (CERES) Energy Balanced and Filled (EBAF) Top-of-Atmosphere (TOA) Edition-4.0 data product. J. Clim. 31 (2), 895–918. https://doi.org/10.1175/JCLI-D-17-0208.1.

Lorenz, R.D., Lunine, J.I., Withers, P.G., McKay, C.P., 2001. Titan, Mars and Earth: entropy production by latitudinal heat transport. Geophys. Res. Lett. 28 (3), 415–418. https://doi.org/10.1029/2000GL012336.

McPhaden, M.J., Zebiak, S.E., Glantz, M.H., 2006. ENSO as an integrating concept in Earth science. Science 314 (5806), 1740–1745. https://doi.org/10.1126/science.1132588.

Meehl, G.A., Covey, C., Delworth, T., Latif, M., McAvaney, B., Mitchell, J.F.B., Stouffer, R.J., Taylor, K.E., 2007. The WCRP CMIP3 multimodel dataset: a new era in climate change research. Bull. Am. Meteorol. Soc. 88 (9), 1383–1394. https://doi.org/10.1175/BAMS-88-9-1383.

Myhre, G., Shindell, D., Bréon, F.-M., Collins, W., Fuglestvedt, J., Huang, J., Koch, D., Lamarque, J.-F., Lee, D., Mendoza, B., Nakajima, T., Robock, A., Stephens, G., Takemura, T., Zhang, H., 2013. Anthropogenic and natural radiative forcing. In: Stocker, T.F., Qin, D., Plattner, G.-K., Tignor, M., Allen, S.K., Boschung, J., Nauels, A., Xia, Y., Bex, V., Midgley, P.M. (Eds.), Climate Change 2013: the Physical Science Basis. Cambridge University Press, Cambridge, UK, pp. 659–740.

NASA Langley Research Center, 2023. CERES Energy Balanced and Filled (EBAF) Ed4.2 data quality summary. Available: https://ceres.larc.nasa.gov/documents/DQ_summaries/CERES_EBAF_Ed4.2_DQS.pdf.

Paltridge, G.W., 1975. Global dynamics and climate - a system of minimum entropy exchange. Quart. J. Roy. Meteor. Soc. 101 (429), 475–484. https://doi.org/10.1002/qj.49710142906.

Reis, A.H., Bejan, A., 2006. Constructal theory of global circulation and climate. Int. J. Heat Mass Tran. 49 (11–12), 1857–1875. https://doi.org/10.1016/j.ijheatmasstransfer.2005.10.037.

Stevens, B., Bony, S., 2013. What are climate models missing? Science 340 (6136), 1053–1054. https://doi.org/10.1126/science.1237554.

Talley, L., Pickard, G., Emery, W., Swift, J., 2011. Descriptive Physical Oceanography: an Introduction, sixth ed. Academic Press, Boston, MA.